Off-body UWB Channel Characterisation within a Hospital Ward Environment

Abstract: Received signal strength measurements and delay statistics are presented for both a stationary and mobile user equipped with a wearable UWB radio transmitter within a hospital environment. The measurements were made for both waist and chest mounted antennas using RF-over-fibre technology to eliminate any spurious electromagnetic scattering effects associated with metallic co-axial cables. The results show that received signal strength values were dependent on whether transmit and receive antennas had line of sight and were also affected by body-shadowing and antenna-body position. For mobile conditions, received signal strength tended to be lognormally distributed with non line of sight links having significantly lower mean values. Excess time delay results for mobile user tests were best described by the Weibull distribution. Overall, the results favoured the chest mounted antenna position, with higher mean signal levels, reduced mean excess delay and less difference between line of sight and non line of sight channels.

Keywords: Ultra-wideband communication; UWB; body-centric communication; off-body; wearable; antennas; statistical channel characterisation; channel sounding; healthcare; medical applications.

1 Introduction

As the quality of healthcare in the western world increases, its success brings a new set of problems. People are living longer; in the US alone the number of people aged 65 years or older increased from 35 million in July 2000 to 39 million in July 2008 (USCB, 2008). The cost of health care for this aging population continues to rise and is causing a strain on the clinical resources of many countries. One way this problem can be addressed is by the use of technology and it is considered that robust high-speed wireless information access will become fundamental in delivering modern and future health care provision (Taparugssanagorn et al., 2009).

It is current practice to monitor hospital patients by positioning medical sensors on specific areas of the patient's body and then connecting each of these sensors to the necessary machines via wiring to enable the processing and display of the data in a meaningful and timely manner. Such data may include vital signs such as respiration rate, oxygen saturation and electrocardiogram. However, the use of cables may complicate treatment and increase interruption during transportation of patients, including a break in essential monitoring (Paksuniemi et al., 2005). Therefore, wireless networking technology can be used to address these issues, with wide ranging benefits including an increase in clinician convenience, patient mobility and comfort. Furthermore, wireless technology can be used to record and relay vital signs or kinematical data for the infirm in their own home to promote independent living (Taparugssanagorn et al., 2009).

Medical wireless connectivity typically involves a body sensor area network and wireless link between the network and the hospital's communication network (Figure 1). The transmission of data from the wireless sensor nodes to the hospital network is an area that has attracted much recent interest (Shin et al., 2007;

Karlsson et al., 2005) with a range of wireless data transmission technologies being employed including Wi-Fi, Zigbee and Bluetooth (Elgharably et al., 2008). However, for link distances below 15 m ultra-wideband (UWB) transmission offers very low power, cost, complexity and very high data rates (Oppermann, 2004). In medical applications, UWB would be suitable for transmitting sizable volumes of streamed patient data within indoor hospital environments as it is less affected by multipath propagation than other competing technologies. Indeed, UWB prospers in rich multipath environment (Hoff et al., 2003). It is thus suitable for a busy ward environment with furniture and pedestrians blocking the line of sight (LOS) path between transmitter (TX) and receiver (RX). UWB is also hospital safe since FCC and equivalent worldwide regulations ensure devices are subject to controlled power and frequency limitations guaranteeing an extremely low level of emissions (CFR, 2008).

Currently only a few studies have addressed the topic of the characterisation of UWB radio links in hospital environments (e.g., Hentila et al., 2005), and some have also considered wearable terminals (Takizawa et al., 2008; Sani et al., 2008). There have also been a few recent studies into off-body UWB link characterisation (Goulianos et al., 2008, 2009) but these measurements were made in the frequency domain and for stationary nodes only, and were performed either in an anechoic chamber or with a distinctly different environmental layout to that addressed in this paper. Therefore, for the first time, we present a comprehensive characterisation of stationary and mobile off-body UWB channels within the unique cluttered environment of a hospital ward. This research issue is both commercially important and also timely as many companies across the globe are investing considerably in wireless monitors for healthcare applications, often choosing a radio chipset for their product without a full appreciation of the intricacies of the site-specific radio propagation characteristics of their chosen technology. Furthermore, the research has considered the effect of antenna position on the body and, by using the wearable time-domain pulse sounder described in Section 2, has been able to take account of unrestricted, natural user movements. This is in stark contrast to the majority of research in this field which is based on frequency domain, static-measurement sounding campaigns.

Figure 1 Body-centric medical device communications showing the off-body communications link

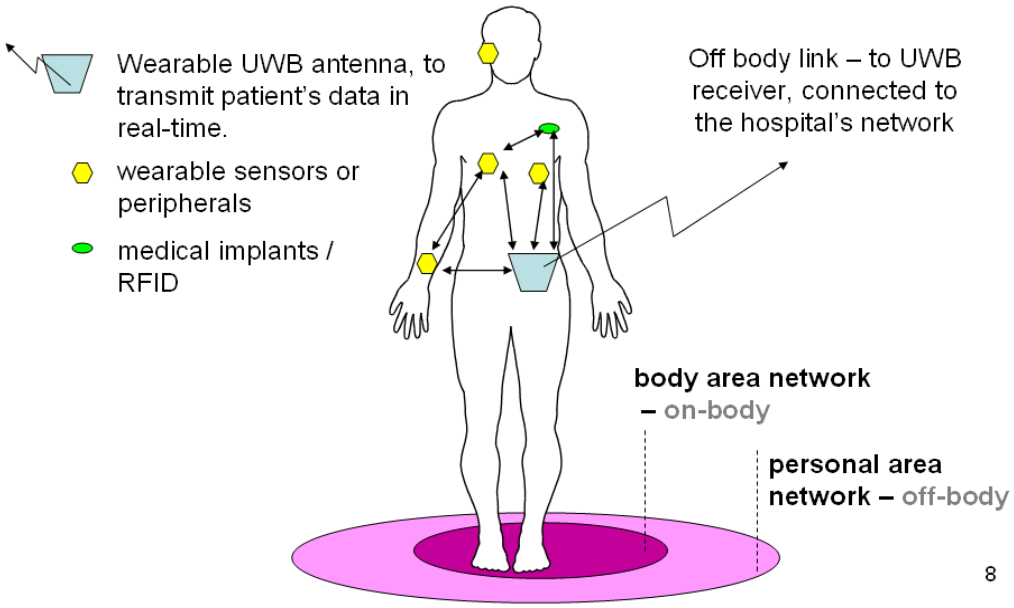

2 Measurement System

The wearable TX (Figure 2) consisted of a single, vertically-polarized UWB antenna (Fractus[1] UM-FR05-S1-P-0-107) connected to a battery-powered UWB PulsON 210[2] source using 1550 nm RF-over-fibre components. The Fractus antenna is a 50 Ω 10 mm^2 chip antenna with an operational bandwidth between 3.1 – 6 GHz. The source was FCC compliant with a centre frequency of 4.7 GHz, a bandwidth of 3.2 GHz and a launch power of –12 dBm. The PulsON UWB system has been utilised previously in (Petroff, 2003; Wong et al., 2006) to undertake UWB channel measurements and indeed was designed for this purpose. The RF-over-fibre system used had a gain of 0 dB and its use eliminated any electromagnetic coupling effects associated with RF co-axial cables traversing the user's body. The presence of such cables has the potential to distort off-body channel measurements by modifying the coupled antenna-body radiation pattern, particularly in non-LOS (NLOS) directions. The RF signal was converted into optical by use of a Miteq optical transmitter[3] (SCMT-100M 6G-28-20-M14) and converted back to RF by a Linear Photonics[4] MiniPR photo-receiver. The signals transmitted off-body were received by a PulsON UWB receiver system using a vertically polarized PulsON UWB antenna connected using standard co-axial cable.

A laptop recorded channel impulse response (CIR) data in the form of a power delay profile (PDP) reported by the PulsON receiver at a rate of 100 samples per second which is sufficient for a 6 GHz node moving at 0.5 ms^{-1} (the Doppler frequency for such a mobile transmitter is 10 Hz). Since each PDP can be post-processed to remove the effect of the measurement system (refer to Section 3), analysis of the results can be related to any non-specific UWB system. The time dispersion captured in each PDP can vary considerably across different UWB radio channels due to three basic mechanisms of NLOS radio propagation: reflection, diffraction and scattering (Laitinen, 1999). All three phenomenon cause distortions of the radio signal and, when the transmitted signal propagates along more than one path to the receiver, multipath occurs. As a result the power received can vary considerably at various locations within the environment (Bultitude et al., 1998) and in an UWB system causes inter-symbol interference which limits the maximum data rate (Rappaport, 1996). Statistical parameters such as mean excess delay and RMS delay spread can be derived from PDPs to describe the temporal spread (time dispersion) of the radio channel (Ho et al, 1994). Mean excess delay, t_{mean}, is the first central moment of the PDP and can be given as:

$$t_{mean} = \frac{\sum_{i=0}^{\infty} t_i P(t_i)}{\sum_{i=0}^{\infty} P(t_i)} \qquad (1)$$

and RMS time delay as:

$$t_{RMS} = \sqrt{\sum_{i=1}^{L} (t_i - t_{mean})^2 \left|h(t, t_i)\right|^2} \quad \text{or} \quad t_{RMS} = \sqrt{\frac{\sum_{i=0}^{\infty} (t_i - t_{mean})^2 P(t_i)}{\sum_{i=0}^{\infty} P(t_i)}} \qquad (2)$$

where t_i is the excess time delay of the i^{th} path and $P(t_i)$ is the Channel impulse response.

[1] http://www.fractus.com/main/fractus/srw_3.1/
[2] http://www.timedomain.com/pulson.php
[3] http://amps.miteq.com/datasheets/MITEQ-SCM_-100M6G.PDF
[4] http://www.linphotonic.com/documents/DataSheets/MPR0118.pdf

The mean excess delay expresses the average propagation delay relative to the first-arriving signal component (Andersen, 1995). The RMS delay spread is the square root of the second central element of the PDP, and thus a measure of the temporal spread of the PDP about the mean excess delay. To prevent noise from affecting calculated delay statistics, a threshold is incorporated into the signal processing software to give most accurate results for t_{mean} and t_{RMS} values.

Figure 2 Wearable UWB transmitter a) antenna and amplifier unit on user's waist showing optical feed, b) block diagram

(a) 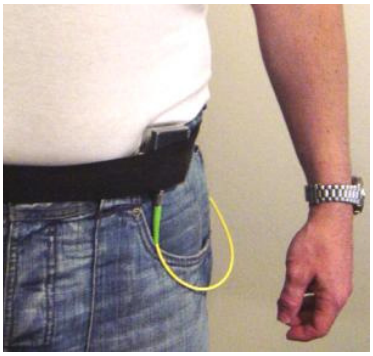 (b) 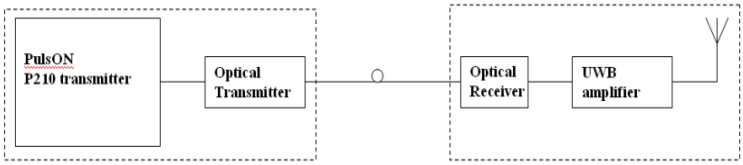

3 Measurement environment and procedure

The measurement campaign was undertaken in a 49 m^2 specialist nurse training room (Figure 3) that faithfully recreates a real hospital ward and it is fitted with regulation specification beds, rails, bedside cabinets, etc. The building was of 1960's construction, consisting mainly of double concrete-block cavity external walls, single brick internal walls and concrete floor. A suspended ceiling supports luminaries at 2.8 m above floor level. This would be in keeping with many established hospitals.

The receiver was placed between beds #2 and #3 at a height of 2.2 m to represent a base-station access point. The wearable transmitter was positioned at the user's waist (1.05 m above floor level) and the chest (1.4 m) with the antenna held against the body using an adjustable synthetic elastic band to minimise body-antenna separation during testing. For waist tests belts and all metallic items such as coins etc. were removed from the user to ensure no distortion of results occurred. The test user was an adult male of mass 82 kg, height 1.78 m. A reference measurement was recorded for a direct LOS link at a TX-RX separation of 3.2 m, as required by the PulsON system to establish an accurate datum. This allowed the CIR to be de-convolved from the time domain pulse recording made at the receiver taking account of the pulse distortion caused by both the transmit and receive chains and antennas. It should be noted that the reference CIR was truncated after the arrival of the first pulse to remove the effect of any multipath signals.

Tests were split into 2 categories: user stationary and user mobile with received signal strength and PDP being recorded in each test. The mobile tests were either LOS or NLOS depending on the orientation of the user. All tests were conducted for a waist worn transmit antenna, and then repeated for a chest-worn transmit antenna to investigate the effect of wearable antenna positioning. The stationary tests were recorded at positions #2 and #6 and involved the user standing beside the bed, sitting on the chair, sitting on the bed or lying (face-up) in the bed. For the mobile tests the user walked smoothly at an approximate speed of 0.5 ms^{-1} along four 5 m

long paths as shown in Figure 3(a): AB (LOS – red path 1); BA (NLOS – red path 2), CD (LOS – green path 1) and DC (NLOS – green path 2).

Note that all tests, except for those for the user in a bed, were carefully planned to be as representative as possible in that they were applicable for either a patient or a clinician wearing a UWB data terminal. The received power profiles were calculated from the recorded CIR samples using Matlab. The study of received power is of interest as it gives an understanding of typical path loss characteristics for off-body links in the ward environment, taking into account all relevant factors including body-interaction effects and shadowing caused by furniture and fittings.

Figure 3 Measurement environment (a) floor plan layout and test paths, and (b) photograph taken from point D toward Bed 1.

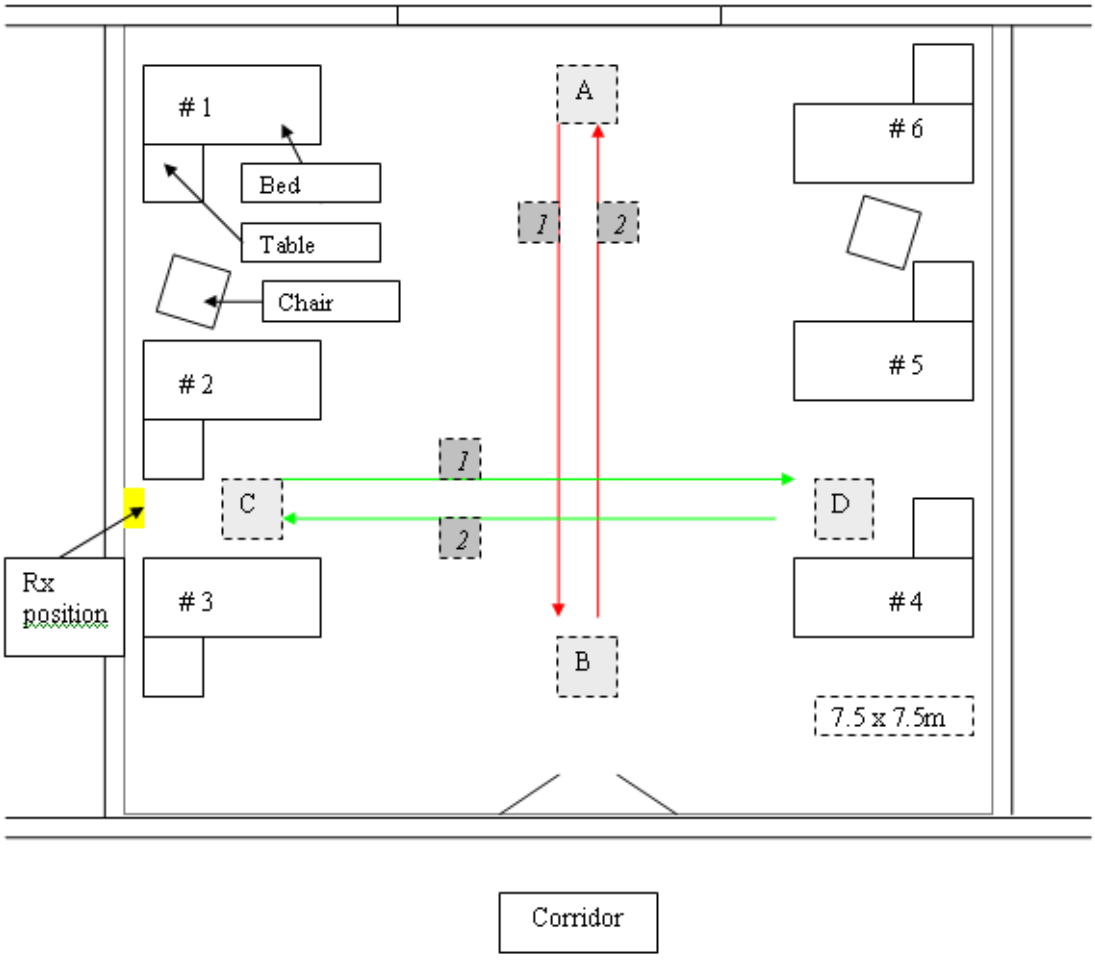

(a)

(b) 

4 Results

4.1 User effects

To investigate the effects of having the antenna worn by a person versus a free standing antenna both received power and excess time delay were characterised in a medium sized room (4 m x 4 m) with minimal furniture and almost identical construction to the hospital ward. The receive antenna was positioned on one of the walls at a height of 2.2 m from the floor and 2 m from each side wall. The transmit antenna was positioned at a height of 1.4 m from the floor for each of the three recordings and also 2 m from each side wall. The TX-RX separation was 3 m.

The results in Table 1 show that the presence of body has a marked effect on received power and excess delay and therefore previous work without the body is not sufficient for characterising the off-body radio channel for medical applications. The difference between LOS and NLOS path loss was around 10 dB and when the antenna was bodyworn the body acted to modestly increase the gain of antenna in the LOS direction. Interestingly, lower mean delays were obtained for the bodyworn LOS case presumably as the user's body reduced the angular spread of the transmitted signal. Likewise, delay spread was increased for the NLOS case as the link must rely on longer propagating paths such as reflections off the walls and creeping waves around the user's body. These results reflect the findings of (Pradabphon et al., 2005) who reported that body-shadowing for an indoor radio link noticeably lowers the received power level.

Table 1 Results of antenna-body tests characterising the effect of the user

	Bodyworn LOS	Bodyworn NLOS	isolated antenna
Received power (dBm)	–62.4	–72.1	–63.7
t_{mean} **(ns)**	19.9	46.2	21.8
t_{RMS} **(ns)**	15.7	53.2	27.4

4.2 User stationary

Table 2 shows received power measurements for the user stationary scenarios outlined in Section 3. A standing position ensured the highest signal levels in all cases, with the lowest values occurring when the user was seated in a chair for the waist-worn antenna and lying down on bed for the chest-worn antenna. This is because when the user was seated, the waist-worn antenna suffered from increased body-shadowing effect, increased TX/RX height differential and also signal blocking due to the metal beds between the seat and the receiver. The chest-worn antenna for the lying position suffered from increased TX/RX height differential and by the change in polarization of the transmitter antenna with respect to that of the receive antenna.

It was also noted that the mean received power at position #6 was higher than at #2, despite the latter being much closer to the receiver (#6 was 7.3 m from the RX, while #2 was only 1.9 m away). This is directly related to position #2 being NLOS (patient facing away from the receiver thus blocking the signal path), whereas position #6 was direct LOS.

Table 2 Received power results for stationary waist and chest tests

Ward location	Patient position	Received Power (dBm)
Waist #2	Standing	–70.5
	Sitting (chair)	–75.8
	Sitting (bed)	–70.8
	Lying (bed)	–74.8
Waist #6	Standing	–69.2
	Sitting (chair)	–73.9
	Sitting (bed)	–69.5
	Lying (bed)	–72.9
Chest #2	Standing	–66.6
	Sitting (chair)	–68.3
	Sitting (bed)	–67.7
	Lying (bed)	–71.4
Chest #6	Standing	–66.5
	Sitting (chair)	–70.9
	Sitting (bed)	–69.3
	Lying (bed)	–72.5

Received power values were generally higher for the chest than the waist at both positions (#2 and #6) because of the higher elevation and the nature of the environment in that most of the room furniture is approximately of waist height which increases signal reflection and scattering. It is also noted that the received power at position #6 is higher than at #2 for the waist-worn antenna, but the reverse is true for the chest-worn antenna. This is related to better positioning of the transmit antenna to reduce body-shadowing

effects. These findings concur with work by (Irahhauten et al., 2005) who found that received power increased as the Tx-Rx height differential decreased.

4.2 User mobile

Examples of received power time series for the user mobile are shown in Figure 4 which includes both waist-worn and chest-worn antenna cases for paths BA (NLOS) and CD (LOS). Each time series was transformed into a cumulative density function (CDF) using bins assigned according to the Freedman-Diaconis rule. Each CDF was then compared to a number of major theoretical distributions to assist in the modelling of the UWB channel, including Rician, Rayleigh, Weibull, Nakagami, Normal, Lognormal, Gamma, etc. The best fit in each case was chosen by using a combination of maximum likelihood parameter estimation within Matlab and inspection which was essential for cases where the lower tail of the empirical CDF was not well modelled by the estimated distribution parameters.

Figure 4 Received power time series for waist and chest worn antenna for journey (a) BA, (b) CD

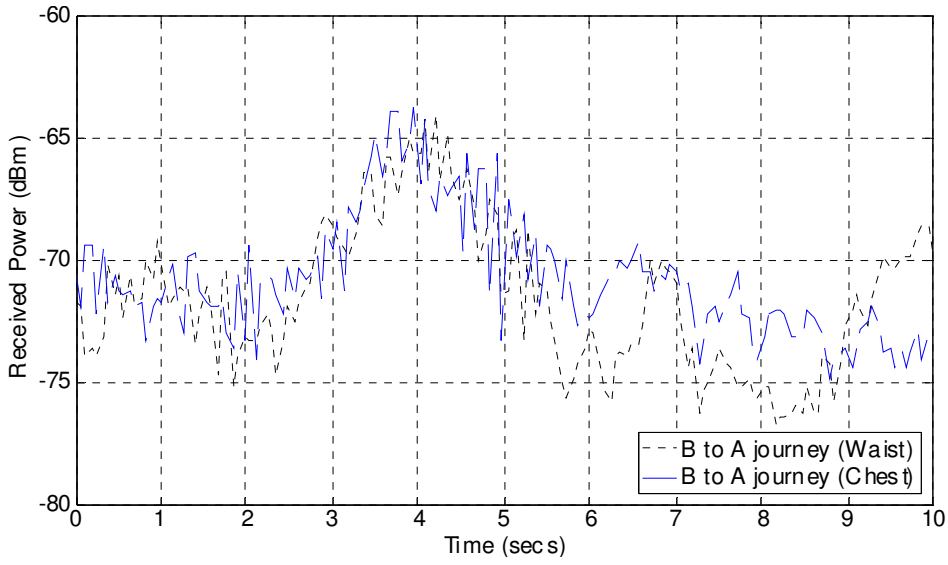

(a)

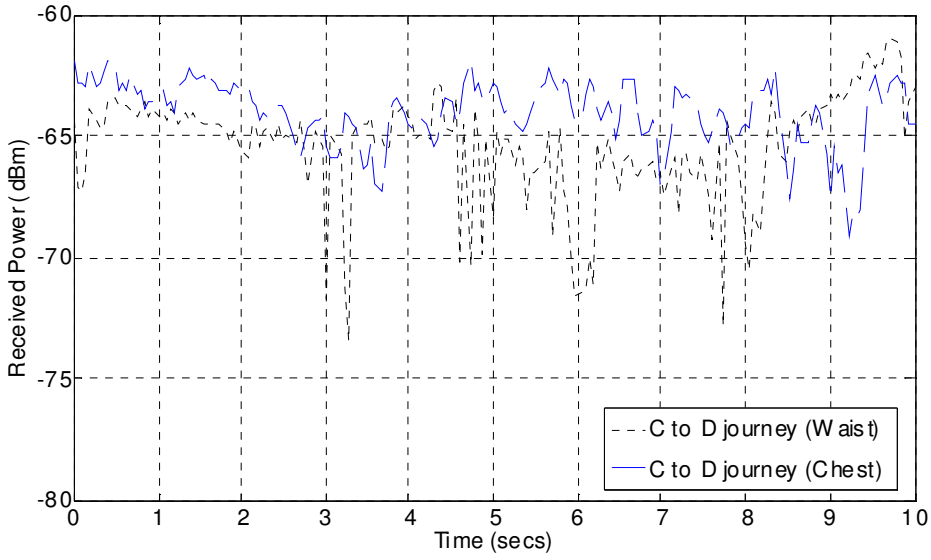

(b)

Figure 5 CDF for waist and chest-worn antennas for paths (a) AB, (b) BA, (c) CD, (d) DC

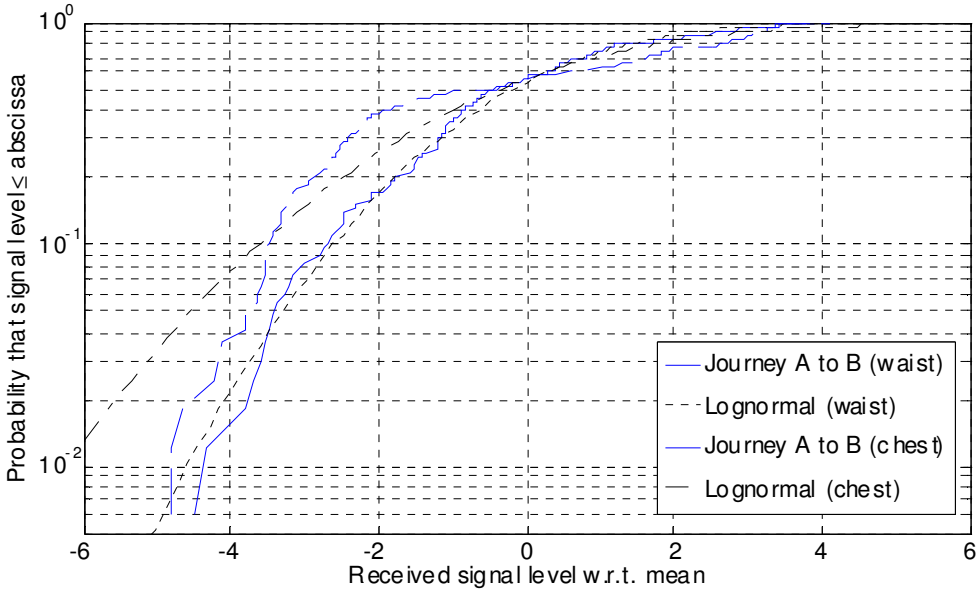

(a)

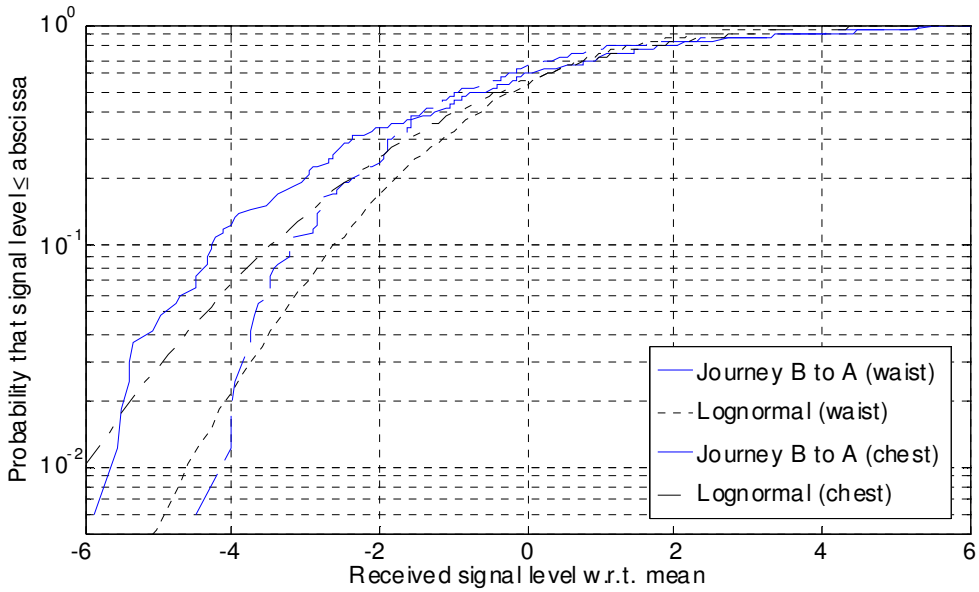

(b)

(c)

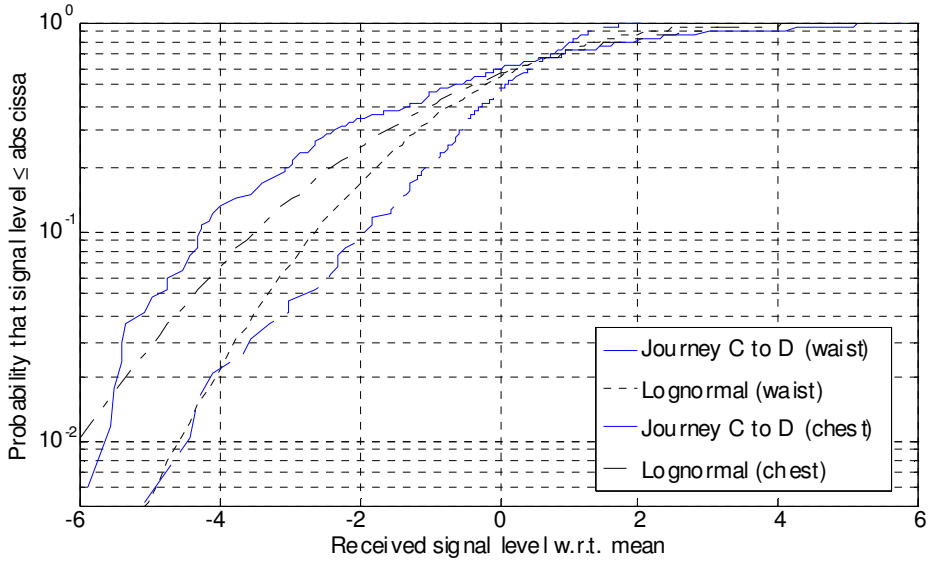

(d)

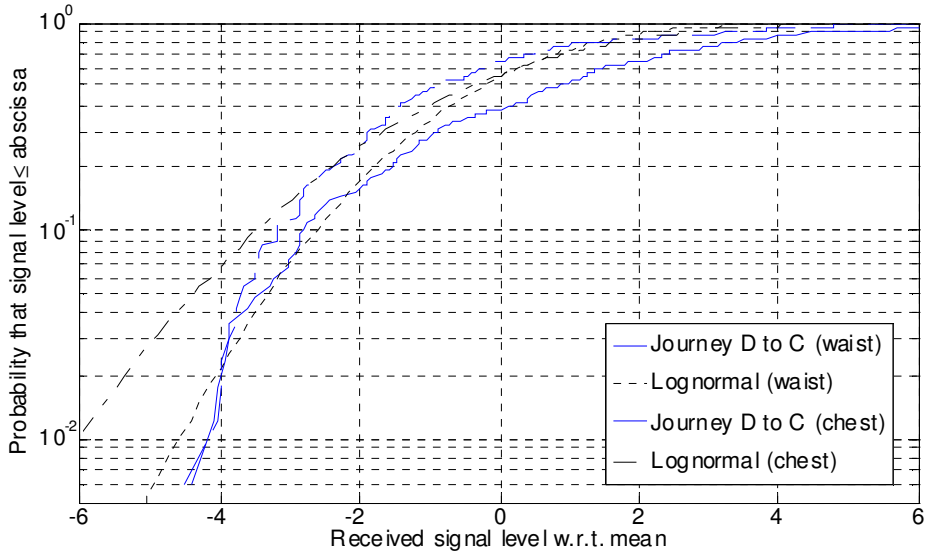

Overall, it was found that the lognormal distribution was the best compromise fit across all paths for both waist- and chest-worn antennas. Nonetheless, there are differences in the details for each path, as shown in Tables 3 and 4. The path-specific lognormal distribution parameters are given in Table 5. Recent work by (Goulianos et al., 2009) reported that received power CDFs were best described by Lognormal distributions, however, that work was conducted in an office environment and was carried out using frequency domain channel sounding from 3.5–6.5 GHz. For the waist-worn antenna, the highest mean power was recorded for path CD and the lowest mean power for path DC. Furthermore, the dominant factor in the tests was whether the antennas were in LOS; there is on average 6.6 dB difference between NLOS and LOS paths for the waist-worn antenna. Dynamic range was found to be around 12 dB for all paths except AB which was only 8.5 dB. Similar results were obtained for the chest-worn antenna with highest mean power recorded for path CD, lowest mean power for path DC. There was on average 4.9 dB difference between NLOS and LOS paths. Dynamic range was again around 12 dB for all paths, except for AB which was 8.9 dB. However, the main difference between the antenna positions was that the difference between LOS and NLOS was notably higher for the waist-worn antenna than for the chest-worn antenna.

Table 3 Link characteristics for waist-worn antenna mobile tests

Path [all dB]	AB LOS	BA NLOS	CD LOS	DC NLOS
Mean	–65.8	–71.4	–65.3	–72.8
Std dev	1.8	2.8	2.2	2.6
Max	–61.7	–64.1	–60.9	–66.3
Min	–70.2	–76.8	–73.3	–79.0
Range	8.5	11.7	12.4	12.7
LOS vs. NLOS		5.6		7.5

Table 4 Link characteristics for chest-worn antenna mobile tests

Path [all dB]	AB LOS	BA NLOS	CD LOS	DC NLOS
Mean	–66.9	–70.8	–65.3	–71.2
Std dev	2.5	2.4	2.5	3.4
Max	–62.4	–63.8	–61.8	–65.2
Min	–71.3	–74.8	–73.8	–79.3
Range	8.9	11.0	12.0	14.1
LOS vs. NLOS		3.9		5.9

Table 5 Lognormal distribution parameters and standard error for each mobile path

		μ		σ	
		Estimate	**Std. Err.**	**Estimate**	**Std. Err.**
Waist antenna	**AB**	1.617	0.008243	0.108	0.005854
	BA	1.296	0.011726	0.162	0.008324
	CD	1.647	0.009202	0.127	0.006532
	DC	1.219	0.01233	0.154	0.008761
Chest antenna	**AB**	1.557	0.011319	0.146	0.008040
	BA	1.332	0.010501	0.140	0.007457
	CD	1.651	0.008177	0.142	0.005796
	DC	1.313	0.01491	0.198	0.010591

In terms of excess delay results, it was found that the Weibull distribution was the overall best fit for both mean delay (t_{mean}) and RMS delay (t_{RMS}) over all paths and for both waist- and chest-worn antennas. The Weibull distribution has been used on a number of occasions to model small-scale fading statistics (Chong and Yong, 2005; Chong et al., 2005; Lim et al., 2006). Studies by (Pradabphon et al., 2005; Goulianos et al., 2009) report that RMS delays were well modelled by Normal distributions. However, both studies were undertaken in office environments with significantly different scattering conditions from this work. Figure 6 shows the delay distributions and the maximum, minimum and mean values of t_{mean} and t_{RMS} are presented in Table 6. The parameters for the path specific Weibull distributions are provided in Table 7. Comparison between the waist- and chest-worn antenna positions for paths AB and BA (Table 6) shows that the differences in t_{mean} and t_{RMS} are negligible. However, for both waist-worn and chest-worn antennas the average t_{mean} and t_{RMS} (delay spread) values were lower for path AB compared to BA, with a similar trend for CD and DC. Indeed, the results in Table 6 highlight that, regardless of user mode, antenna position and direction of travel (LOS or NLOS), the mean values of excess time delay are largely similar with t_{mean} ~ 64 ns and t_{RMS} ~ 66 ns. This is due to the richness of the indoor multipath environment.

Figure 6 Per-path delay distributions (a) t_{mean} for AB, (b) t_{RMS} for AB, (c) t_{mean} for BA, (d) t_{RMS} for BA, (e) t_{mean} for CD, (f) t_{RMS} for CD, (g) t_{mean} for DC, (h) t_{RMS} for DC

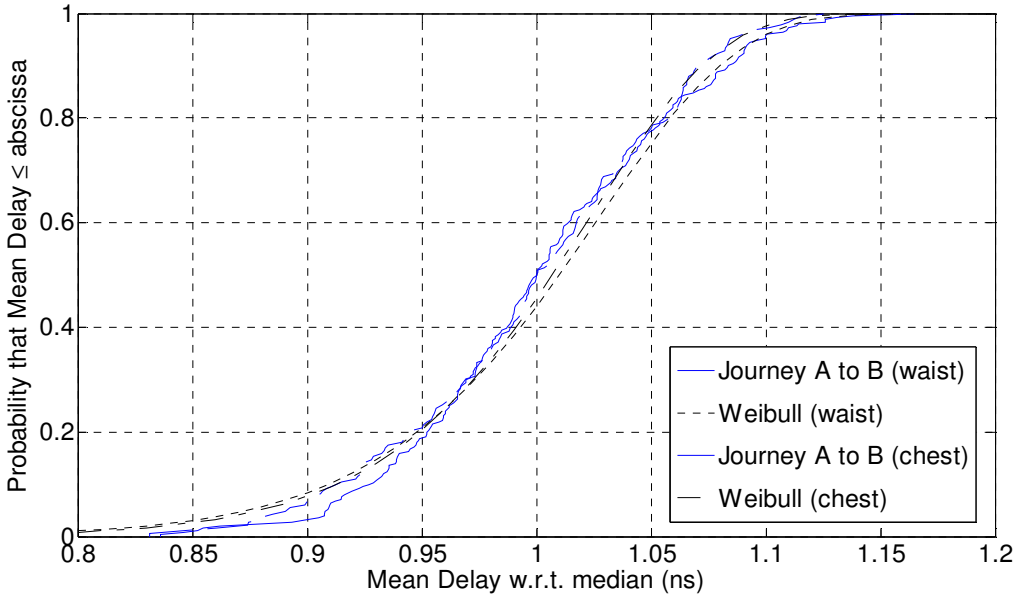

(a)

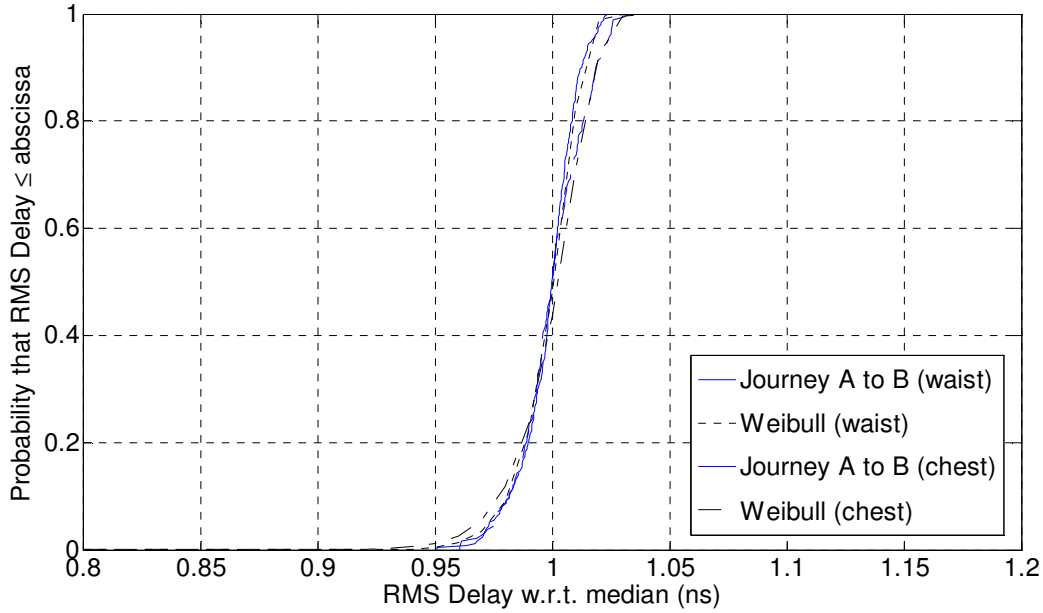

(b)

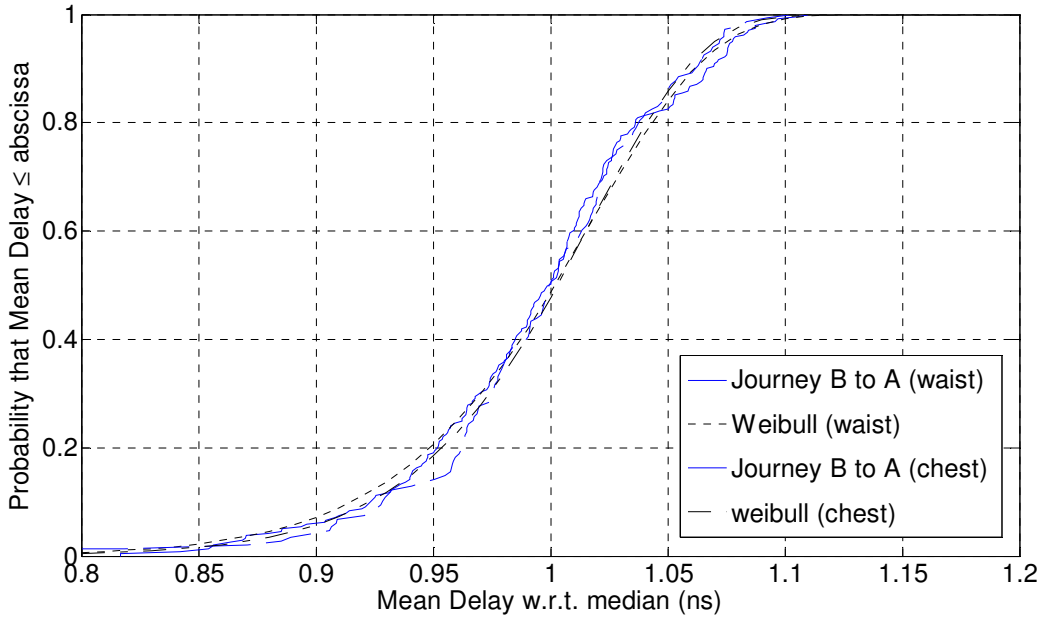
Probability that Mean Delay ≤ abscissa
Mean Delay w.r.t. median (ns)
Journey B to A (waist)
Weibull (waist)
Journey B to A (chest)
weibull (chest)
0
0.2
0.4
0.6
0.8
1
0.8
0.85
0.9
0.95
1
1.05
1.1
1.15
1.2

(c)

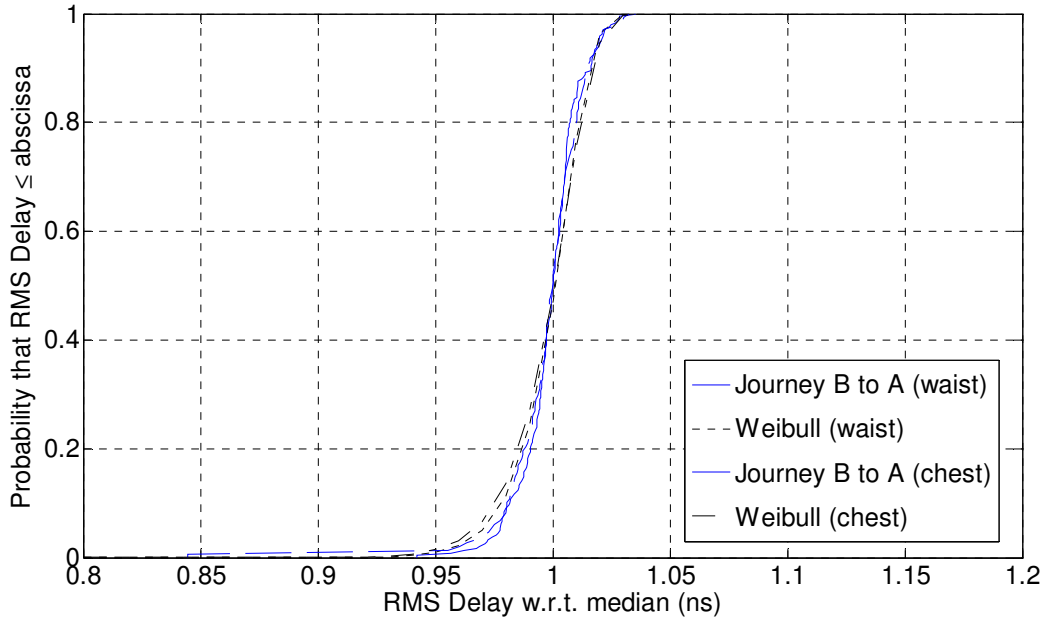
Probability that RMS Delay ≤ abscissa
RMS Delay w.r.t. median (ns)
Journey B to A (waist)
Weibull (waist)
Journey B to A (chest)
Weibull (chest)
0
0.2
0.4
0.6
0.8
1
0.8
0.85
0.9
0.95
1
1.05
1.1
1.15
1.2

(d)

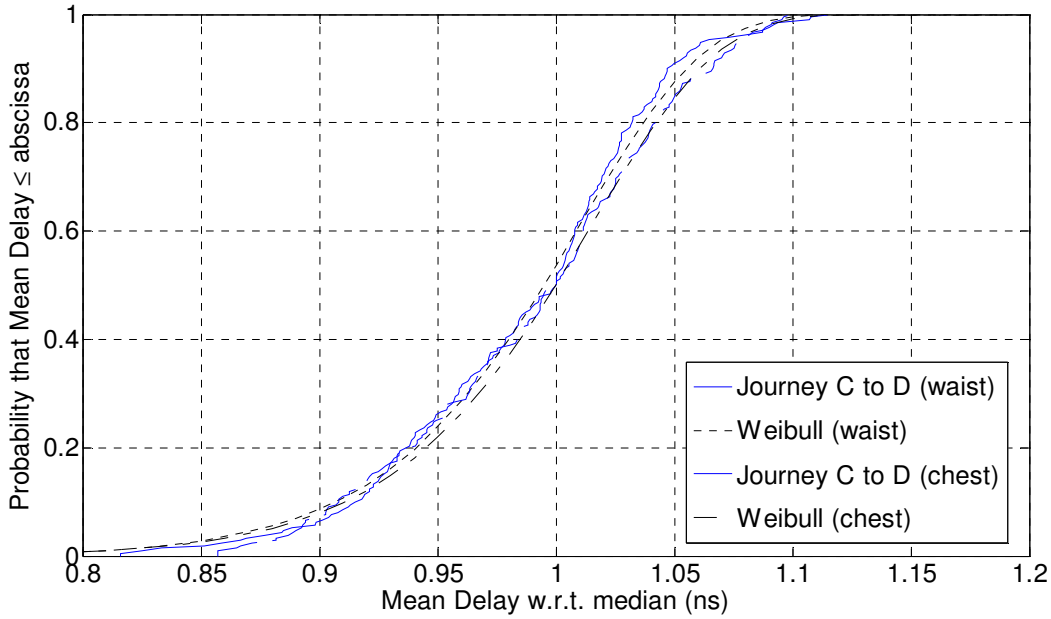
Probability that Mean Delay ≤ abscissa
Mean Delay w.r.t. median (ns)
Journey C to D (waist)
Weibull (waist)
Journey C to D (chest)
Weibull (chest)
0
0.2
0.4
0.6
0.8
1
0.8
0.85
0.9
0.95
1
1.05
1.1
1.15
1.2

(e)

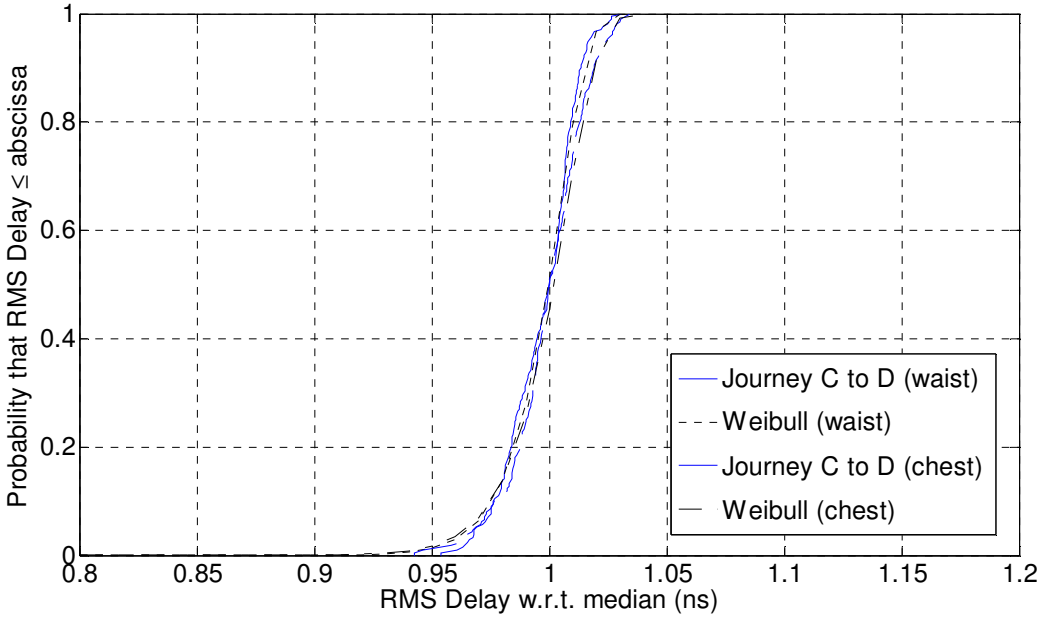
Probability that RMS Delay ≤ abscissa
RMS Delay w.r.t. median (ns)
Journey C to D (waist)
Weibull (waist)
Journey C to D (chest)
Weibull (chest)
0
0.2
0.4
0.6
0.8
1
0.8
0.85
0.9
0.95
1
1.05
1.1
1.15
1.2

(f)

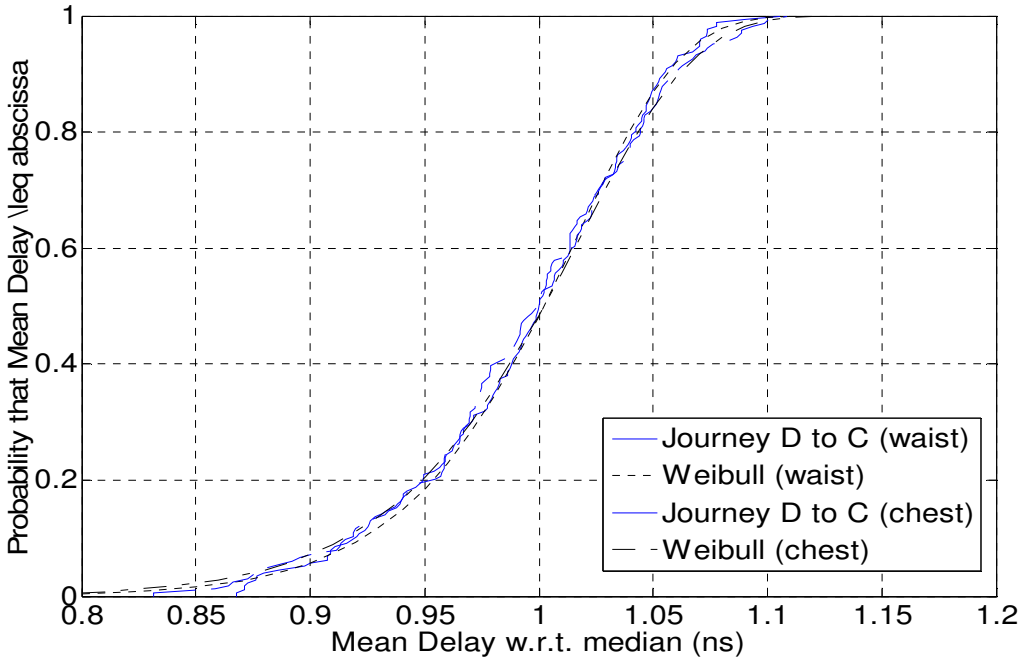
Probability that Mean Delay \leq abscissa
Mean Delay w.r.t. median (ns)
Journey D to C (waist)
Weibull (waist)
Journey D to C (chest)
Weibull (chest)

(g)

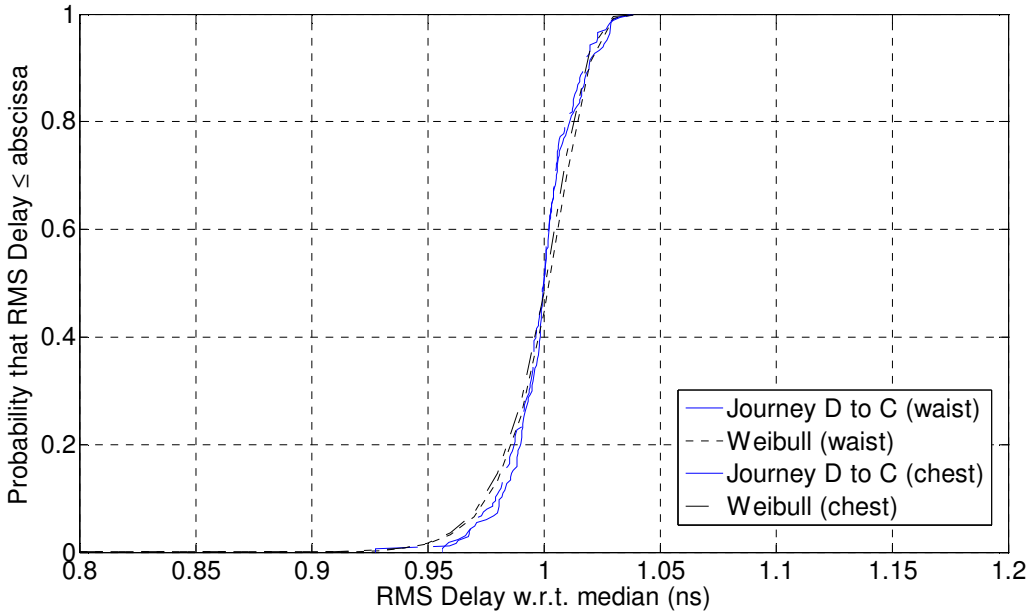
Probability that RMS Delay ≤ abscissa
RMS Delay w.r.t. median (ns)
Journey D to C (waist)
Weibull (waist)
Journey D to C (chest)
Weibull (chest)

(h)

Table 6 Time delay results for user mobile tests

		Waist	Chest
AB	**max t_{mean} (ns)**	73.2	73.7
	mean t_{mean} (ns)	61.2	61.8
	min t_{mean} (ns)	47.1	50.0
	max t_{RMS} (ns)	67.8	67.7
	mean t_{RMS} (ns)	65.6	65.5
	min t_{RMS} (ns)	60.3	61.0
BA	**max t_{mean} (ns)**	72.1	70.9
	mean t_{mean} (ns)	64.6	64.0
	min t_{mean} (ns)	53.1	54.7
	max t_{RMS} (ns)	68.5	68.5
	mean t_{RMS} (ns)	66.1	66.1
	min t_{RMS} (ns)	62.3	63.5
CD	**max t_{mean} (ns)**	71.0	71.3
	mean t_{mean} (ns)	64.1	64.0
	min t_{mean} (ns)	55.4	57.8
	max t_{RMS} (ns)	68.2	68.3
	mean t_{RMS} (ns)	65.9	65.9
	min t_{RMS} (ns)	62.2	63.0
DC	**max t_{mean} (ns)**	74.4	73.1
	mean t_{mean} (ns)	66.0	65.6
	min t_{mean} (ns)	57.6	59.0
	max t_{RMS} (ns)	69.0	68.9
	mean t_{RMS} (ns)	66.4	60.2
	min t_{RMS} (ns)	61.7	62.3

Table 7 Estimated Weibull distribution parameters for each mobile test

			a		*b*	
			Estimate	**Std. Err.**	**Estimate**	**Std. Err.**
Waist	**AB**	t_{mean}	64.84	0.24172	17.94	0.83796
		t_{RMS}	66.28	0.04596	96.14	4.57657
	BA	t_{mean}	66.23	0.21640	20.83	1.02258
		t_{RMS}	66.52	0.05484	82.75	3.79994
	CD	t_{mean}	64.63	0.23090	20.35	1.05626
		t_{RMS}	66.12	0.06130	78.45	4.09045
	DC	t_{mean}	65.44	0.23734	22.89	1.34228
		t_{RMS}	66.73	0.07801	70.80	4.01682
Chest	**AB**	t_{mean}	65.64	0.26750	19.16	1.08845
		t_{RMS}	66.44	0.06882	75.58	4.18124
	BA	t_{mean}	65.63	0.25027	22.68	1.43635
		t_{RMS}	66.37	0.07687	74.76	4.53565
	CD	t_{mean}	65.78	0.23600	20.27	1.08460
		t_{RMS}	66.40	0.06903	70.00	3.62214
	DC	t_{mean}	67.59	0.23473	22.90	1.34220
		t_{RMS}	66.86	0.07518	70.95	3.86312

4.3 Rotation test

A rotation test was performed to further investigate the differences in signal propagation from the two candidate antenna mounting positions on the user's body. Initially, the user (and transmit antenna) were directly facing the receiver module. The user then rotated at a constant speed with a rotation time of 20 s. The received power time series for both antenna positions is shown in Figure 7. The results show a difference of ~10 dB in received power between LOS and NLOS conditions. Overall, the received power time series for waist- and chest-worn antennas were similar, but with one notable difference: the chest-worn antenna experienced a marked increase in received signal power between 10 to 15 seconds which the waist-worn antenna did not. The excess delay results for the rotation test are summarised in Table 8. Both t_{mean} and t_{RMS} values for the waist-worn antenna are slightly higher than for the chest-worn antenna. These results may be attributed to the different scattering environment experienced by each antenna mounting point with the waist-worn antenna suffering from an increased level of clutter at that height above the floor level.

Figure 7 Received power time series for user rotating

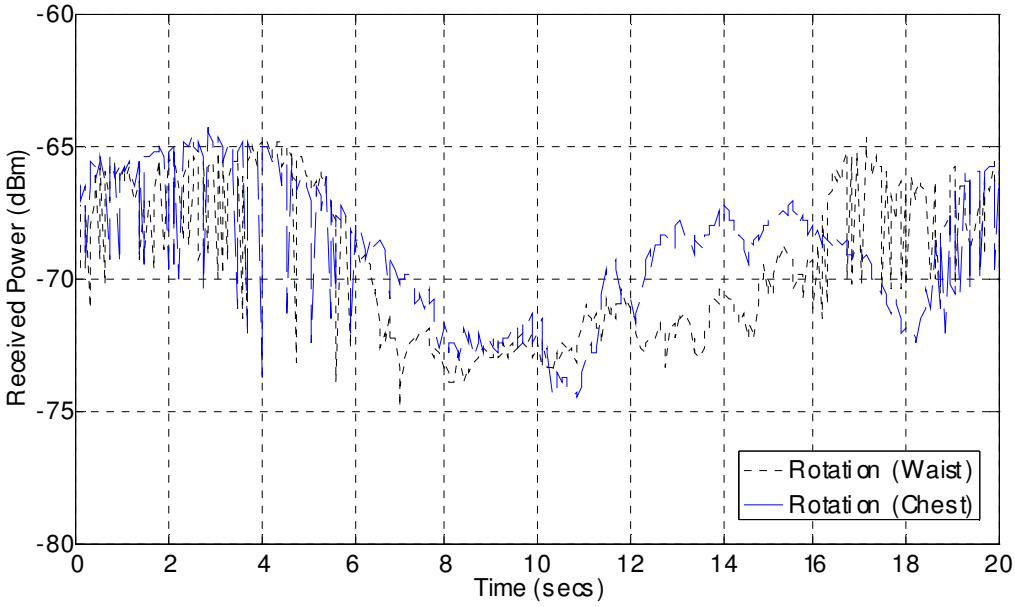

Table 8 Time delay results for rotation tests

	Waist	**Chest**
max t_{mean} **(ns)**	72.9	71.4
mean t_{mean} **(ns)**	63.6	62.6
min t_{mean} **(ns)**	50.7	50.2
max t_{RMS} **(ns)**	68.6	68.8
mean t_{RMS} **(ns)**	66.0	65.7
min t_{RMS} **(ns)**	63.1	61.5

5 Conclusions

Relative path loss results and delay statistics for both the stationary and mobile off-body UWB radio channel have been presented. The measurements were made in a realistic hospital ward environment using RF-over-fibre technology. The mobile results show that the variation in total received power for a waist-worn and also chest-worn transmitter are generally well described by a lognormal distribution, but that the mean levels and dynamic range were dependent on the nature of the path and line of sight conditions. The time delay results for the mobile tests showed that for both the waist- and chest worn antenna the Weibull distribution offered the best general fit. The maximum and minimum delay values were recorded for the waist-worn antenna position, although such is the richness of the multipath environment that many of the t_{mean} and t_{RMS} values had only limited dissimilarity.

Stationary experiments highlighted that received power was dependent on user orientation as well as the multipath hospital environment. Rotation experiments highlighted that received power was dependant on

antenna positioning on the body, body shadowing effects and alignment with scattering objects and surfaces within the environment. The delay statistics for the rotation experiments indicate that both t_{mean} and t_{RMS} values for the waist-worn antenna are slightly higher than for the chest-worn antenna. Also, t_{mean} and t_{RMS} values rise with increased body shadowing.

In all cases it was evident that the chest-worn antenna arrangement had discernibly lower average mean excess delay (t_{mean}) and RMS delay (t_{RMS}) values compared to the waist-worn antenna. For both the stationary and rotation measurements the chest-worn antenna arrangement also showed higher received power levels. For a mobile user, the chest-worn antenna arrangement had higher mean received power values for NLOS, and, perhaps more importantly, there was also less difference in levels for LOS scenarios compared to NLOS. Therefore, future work will extend the work to consider a wider range of antenna mounting positions and will also investigate the effect of mobile scatterers such as pedestrians on these off-body links.

References

Andersen, J.B., Rappaport, T.S. and Yoshida, S. (1995) 'Propagation measurements and models for wireless communications channels', *IEEE Communications Mag.*, Vol. 33, Issue 1, pp.42–49.

Bultitude, R.J.C., Hahn, R.F. and Davies, R.J. (1998) 'Propagation considerations for the design of an indoor broad-band communications system at EHF', *IEEE Trans. Vehicular Technology*, Vol. 47, 1, pp.235–245.

Chong, C. C., and Yong, S. K. (2005) 'A generic statistical based UWB channel model for high-rise apartments', *IEEE Trans. Antennas and Propagation* (Special Issue on Antennas and Propagation Applications), vol. 53, no. 8, pp.2389–2399.

Chong, C. C., Kim, Y. and Lee, S. S. (2005) 'A modified S-V clustering channel model for UWB indoor residential environment', *Proc. IEEE Veh. Technol. Conf.* (VTC 2005-Spring), vol. 1, pp. 58-62, Stockholm, Sweden

Code of Federal Regulations (CFR), (2008) Title 47–Telecomms, Chapter I, Part 15-Radio Frequency devices. Sect. 15.517 "Technical requirements for indoor UWB systems", pp. 846–847.

Elgharably, R. et al, (2008) 'Wireless-Enabled Telemedicine System for Remote Monitoring', *Biomedical Engineering Conference, 2008.* CIBEC 2008. Cairo International, pp.1-4.

Goulianos, A. A. et al, (2009) 'Wideband Power Modeling and Time Dispersion Analysis for UWB Indoor Off-Body Communications', *IEEE Transactions on Antennas and Prop.* vol. 57, no. 7, pp. 2162–2171.

Goulianos, A. A., Brown, T., Stavrou, S. (2008) 'A Novel Path-Loss Model for UWB Off-Body Propagation', *IEEE Vehicular Technology Conference*, pp.450–454.

Hentila, L. et al, (2005) 'Measurement and modelling of an UWB channel at hospital', *IEEE Intl. Conf. Ultra-Wideband,* pp.113–117.

Ho, C. M. P., Rappaport, T. S. and Koushik, P. (1994) 'Antenna Effects on Indoor Obstructed Wireless Channels and a Deterministic Image-Based Wide-Band Propagation Model for In-Building Personal Communication Systems', *Intl. Journal of Wireless Information Networks*, pp.61–76.

Hoff, H., Eggers P.C.F. and Kovacs, I.Z. (2003) "Directional indoor ultra wideband propagation mechanisms", *2003 IEEE 58th Vehicular Technology Conf.*, VTC 2003, Vol. 1, pp.188–192.

Irahhauten, Z. et al, (2005) 'UWB channel measurements and results for wireless personal area networks applications', *European Conference on Wireless Technology, 2005*. 3-4 Oct. 2005. pp.189-192.

Karlsson, M. et al, (2005) 'Wireless system for real-time recording of heart rate variability for home nursing', *Proc. 27th Annual IEEE Eng. in Medicine and Biology Conf.*, Shanghai, China, pp.3717–3719.

Laitinen, H. (1999) 'Verification of a stochastic radio channel model using a wideband measurement data', Helsinki University of Technology Master's Thesis,. Available [online]: http://www.vtt.fi/tte/rd/propagation/Mthesis.pdf

Lim, C. P. et al, (2006) 'Propagation modeling of indoor wireless communications at 60 GHz', *IEEE Antennas and Propagation Society International Symposium*, pp. 2149–2152.

Oppermann, I. (Ed.), (2004) *UWB theory and application*. Wiley, UK.

Paksuniemi, M. et al, (2005) 'Wireless sensor and data transmission needs and technologies for patient monitoring in the operating room and intensive care unit', *Proc. 27th Annual IEEE Eng. in Medicine and Biology Conf.,* Shanghai, China, pp. 5181–5185.

Petroff, A. et al, (2003) 'PulsON P200 UWB radio: simulation and performance results', *2003 IEEE Conference on Ultra Wideband Systems and Technologies,* pp.344–348.

Pradabphon, A. Et al (2005). 'Experimental evaluation scheme of UWB propagation channel with human body', *IEEE Intl Symposium on Communications and Information Technology, 2005. ISCIT 2005.* Vol. 1, 12-14 Oct. pp.660-663.

Rappaport, T.S. (1996) *Wireless communication: Principles and practice*, Prentice Hall.

Sani, A. et al, (2008) 'Time domain characterisation of ultra wideband wearable antennas and radio propagation for body-centric wireless networks in healthcare applications', *5th Intl. Workshop Wearable & Implantable Body Sensor Networks (BSN 2008)*, Hong Kong.

Shin, D. I., Huh, S. J. and Pak, P. J. (2007) 'Patient monitoring system using sensor network based on the ZigBee radio', 6th *Intl. Conf. Information Technology Applications in Biomedicine*, Tokyo, pp.313–315.

Takizawa, K. et al, (2008) 'Channel models for wireless body area networks,' *Proc. 30th Annual IEEE Eng. in Medicine and Biology Conf.*, pp.1549–1552.

Taparugssanagorn, A. et al, (2009) 'UWB channel modeling for wireless body area networks in medical applications,' *3rd Intl. Symp. Medical Info. & Comm. Tech.*, Montreal, Canada. p5.

USCB (2008) - U.S. Census Bureau - Population Division, 'Annual Estimates of the Resident Population by Sex and Five-Year Age Groups for the United States: April 1, 2000 to July 1, 2008', (NC-EST2008-01).

Wong, S.S.M. et al, (2006) 'Propagation characteristics of UWB radio in a high-rise apartment', *8th Int. Conf. Advanced Comm. Tech., 2006. ICACT 2006.* Vol. 2, pp.913–918.